JOURNAL OF MATERIALS SCIENCE 28 (1993) 975–981

Mössbauer spectroscopic studies of the crystallization of amorphous $Fe_{80}B_{20-x}Si_x$ ($x=0$, 2, and 8) alloys

R. SINGHAL, U. C. JOHRI, R. M. SINGRU
Department of Physics, Indian Institute of Technology, Kanpur 208 016, India

The crystallization process of amorphous $Fe_{80}B_{20-x}Si_x$ ($x=0$, 2, and 8) ferromagnetic alloys has been studied by using ^{57}Fe Mössbauer spectroscopy and X-ray diffraction studies. Results for samples heat treated at different temperatures for different times show that the crystallization of $Fe_{80}B_{20-x}Si_x$ samples having $x = 0$ and 2 leads to α-Fe and t-Fe_3B, while for $x = 8$, it leads to α-Fe, t-Fe_2B, and perhaps Fe–Si. It is further observed that the addition of silicon to the Fe–B system improves the thermal stability of the system.

1. Introduction

In recent years the amorphous ferromagnetic alloys have been widely investigated because of their interesting primary magnetic properties and potential technical applications. Thus the basic binary magnetic metallic system Fe_xB_{100-x} has been studied extensively with the aim of understanding its structure, physical, and magnetic properties and the kinetics of their crystallization. Later it was found that addition of metalloid element (phosphorus, silicon, etc.) produces a ternary system with improved thermal stability and magnetic properties. In particular, the ternary alloy system Fe–B–Si has been the subject of several studies [1–13].

We have recently studied the temperature dependence of the electrical resistivity of $Fe_{80}B_{20-x}Si_x$ ($0 \leq x \leq 12$) amorphous ferromagnets in the temperature range 8-300 K [14]. Detailed quantitative analysis of these results showed that over and above a dominant structural contribution there exists in these alloys a significant magnetic contribution proportional to $T^{3/2}$ or T^2 depending on the temperature range. High-temperature magnetization studies of $Fe_{80}B_{20-x}Si_x$ ($0 \leq x \leq 12$), carried out in our laboratory, showed that the effect of addition of silicon ($x \geq 4$) induces the crystallization to occur in a two-step process, i.e. for $x = 0$–2, the final crystallized phases are α-Fe and t-Fe_3B, but for $x \geq 4$ the phases are α-Fe and t-Fe_2B [15]. In order to gain a better understanding of the effect of the metalloid silicon on the kinetics of crystallization of these amorphous ferromagnets, we have carried out Mössbauer spectroscopic measurements of $Fe_{80}B_{20-x}Si_x$ ($x = 0$, 2 and 8) samples subjected to different heat treatments. These samples were also studied by X-ray diffraction (XRD) to identify the final crystallized phases. The present results corroborate our earlier conclusions based on high-temperature magnetization studies.

2. Experimental procedure

The amorphous ribbons of $Fe_{80}B_{20-x}Si_x$ ($x = 0$, 2 and 8) were provided by Dr F.E. Luborsky, General Electric Company, USA. Mössbauer absorbers were prepared from these ribbons by placing them parallel and close to each other by pasting them over copper rings having an inner diameter of 1 cm. Using these absorbers and a radioactive ^{57}Co source in a rhodium matrix (Amersham International Limited, Amersham, UK), Mössbauer spectra were recorded at room temperature with a constant acceleration, linear-mode Mössbauer spectrometer coupled to a multichannel analyser. A least-squares curve-fitting computer program using Lorentzian shapes for the peaks was used to determine the Mössbauer parameters. X-ray diffraction studies were performed on the crystallized samples using a Rich and Seifert Isodebyeflex 2002 diffractometer with a CrK_α source.

3. Results and discussion

3.1. Study of as-received samples

The Mössbauer spectra for the as-received $Fe_{80}B_{20-x}Si_x$ ($x = 0$, 2, and 8) samples recorded at room temperature exhibit well-defined but broadened six-line patterns. Such broadened spectral lines are characteristic of amorphous magnetic solids. Mössbauer parameters, obtained by computer analysis, for the as-received $Fe_{80}B_{20-x}Si_x$ samples ($x = 0$, 2 and 8) are listed in Table I. The present results indicate that the isomer shift (IS) increases linearly with increasing silicon concentration, x, for the three values of x studied (Table I). According to Walker *et al.* [16], the IS increases with increasing 3*d*-and decreasing 4*s*-electron numbers for the ^{57}Fe absorber atoms in Mössbauer spectroscopy. In the present case, the replacement of boron by silicon (i.e. the addition of silicon to $Fe_{80}B_{20}$ for $x = 2$ and 8 samples) causes

0022–2461 © *1993 Chapman & Hall*

TABLE I Mössbauer parameters, obtained from computer analysis, for the as-received $Fe_{80}B_{20-x}Si_x$ ($x = 0, 2,$ and 8) amorphous ferromagnets

x (at %)	H (kOe) [a]	IS (mm s^{-1}) [b]	Γ(FWHM) (mm s^{-1}) [c]
0	253	0.07	0.92
2	255	0.09	0.94
8	258	0.16	0.86

[a] Internal magnetic field at ^{57}Fe nucleus, typical error is ± 3 kOe.
[b] Isomer shift with respect to α-Fe, typical error is ± 0.01 mm s^{-1}.
[c] Width of the spectral line, typical error is ± 0.01 mm s^{-1}.

more electrons to fill the $3d$-holes of iron through the hybridization of the $3d$-orbitals of iron with s- and p-orbitals of the metalloid silicon and these surplus $3d$ electrons, in turn, shield more $4s$ electrons thereby reducing the electron density at the nucleus. The observed dependence of IS on x is in agreement with the results of Taniwaki and Maeda [17] on Fe–B–Si alloys.

It is also observed that the internal magnetic field, H, increases slightly with x (Table I) as boron is replaced by silicon. Such a slight increase of H with x agrees with the observations reported by Gonser *et al.* [18]. These authors proposed that the slight increase in H with increasing silicon is due to the strain caused during the replacement of a small metalloid atom by a large metalloid atom in an interstitial site. Similar behaviour of H was observed by Taniwaki and Maeda [17] for $Fe_{80}B_{20-x}Si_x$.

3.2. Study of heat treated samples

3.2.1. $x = 0$

In order to study the kinetics of crystallization in the $Fe_{80}B_{20-x}Si_x$ system, the as-received sample for $x = 0$ was heated at various temperatures listed below (the heating time is shown in parentheses) :300 °C (1 h), 300 °C (2 h), 350 °C (1 h), 350 °C (2 h), 400 °C (1 h), and 400 °C (4 h). Mössbauer spectra of such heat-treated samples were recorded at room temperature. The resulting Mössbauer parameters are listed in Table II. The spectra for the sample heated below 400 °C are shown in Fig. 1 and they consist of six broad lines (linewidth FWHM being 0.9–1.0 mm s^{-1}) typical of the amorphous phase. The $x = 0$ sample, heat treated at 400 °C, shows a dramatic change in the nature of the Mössbauer spectrum indicating the familiar transformation from the amorphous phase to the crystalline phase. The two spectra, (i) 400 ° C (1 h), (ii) 400 °C (4 h) for the $x = 0$ sample, were fitted into four subspectra (Fig. 2). These spectra are characterized by hyperfine fields in four different ranges: 333 kOe (first range), 287–290 kOe (second range), 266–268 kOe (third range) and 224 kOe (fourth range). The first range is associated with the ^{57}Fe probes in a b c c α-Fe-like environment. We propose that the last three ranges are associated with the t-Fe_3B phase in agreement with the observations of Caer and Dubois [19]. It may be pointed out that, in their Mössbauer study of the crystallization of $Fe_{80}B_{20}$ amorphous alloys, Sánchez *et al.* [20] found evidence for a mixture of tetragonal and orthorhombic Fe_3B (t-Fe_3B and o-Fe_3B) for samples annealed at 800 °C. However, in our case, the X-ray diffraction studies of the samples revealed the presence of only α-Fe and t-Fe_3B, and there was no indication of o-Fe_3B. Our Mössbauer analysis shows three distinct hyperfine fields which

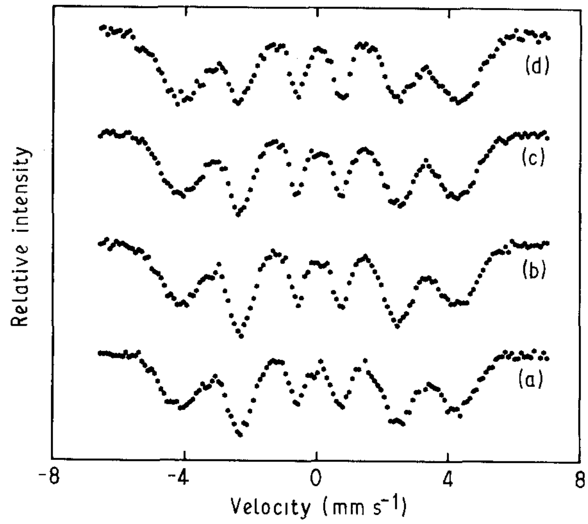

Figure 1 Mössbauer spectra recorded at room temperature of $Fe_{80}B_{20}$, heat treated at (a) 300 °C (1 h), (b) 300 °C (2 h), (c) 350 °C (1 h), (d) 350 °C (2 h).

TABLE II Mössbauer parameters, obtained from computer analysis, for $x = 0$ sample after various heat treatments

Annealing temp. (°C)	Annealing time (h)	IS (mm s^{-1})	H (kOe)	Γ (mm s^{-1})	Remark
300	1	0.08	256	0.92	Amorphous
300	2	0.07	258	0.92	Amorphous
350	1	0.08	259	0.94	Amorphous
350	2	0.08	260	1.0	Amorphous
400	1	(i) 0.00	333	0.28	α-Fe
		(ii) 0.07	290	0.38	t-Fe_3B
		(iii) 0.11	268	0.46	
		(iv) 0.07	224	0.50	
400	4	(i) 0.00	333	0.28	α-Fe
		(ii) 0.10	287	0.42	t-Fe_3B
		(iii) 0.12	266	0.44	
		(iv) 0.07	224	0.50	

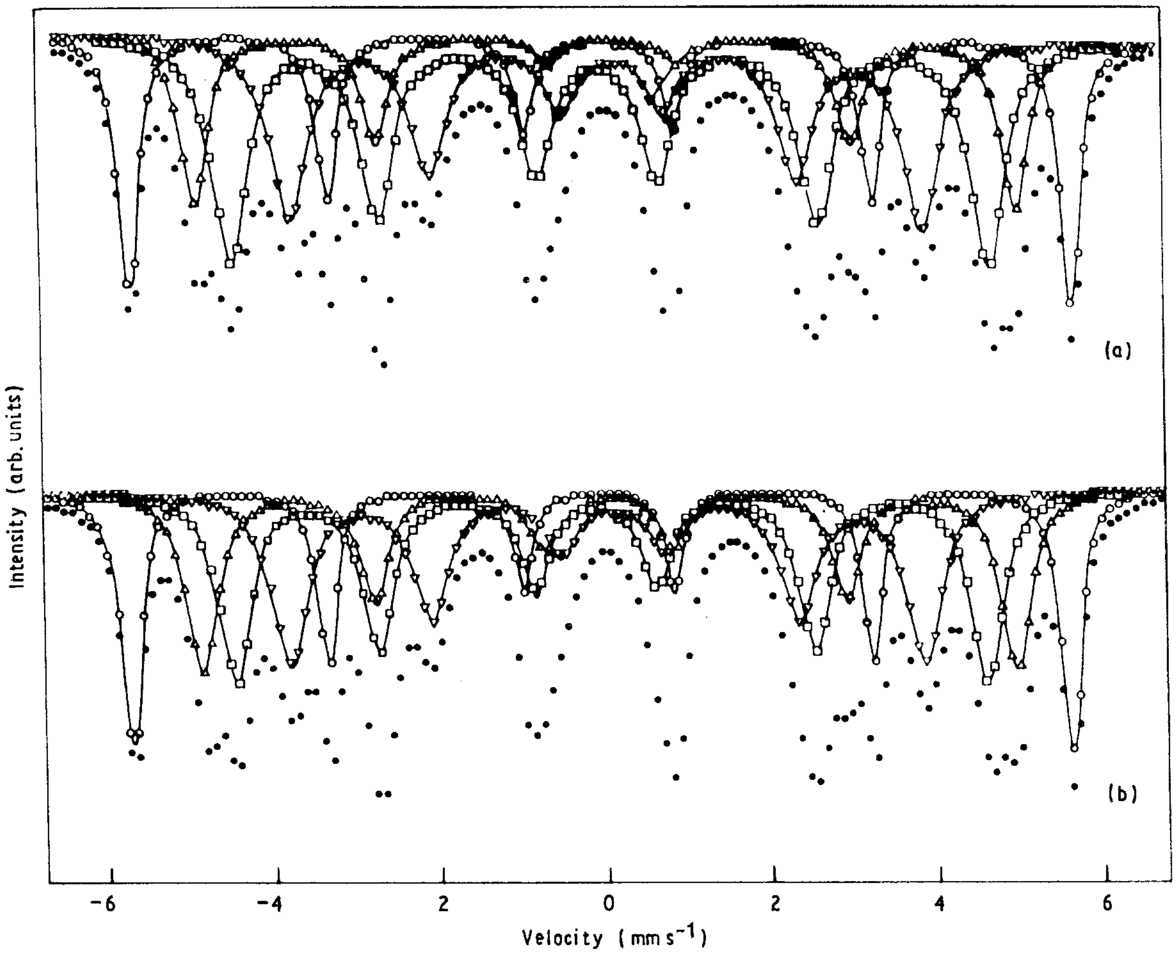

Figure 2 Mössbauer spectra recorded at room temperature of $Fe_{80}B_{20}$, heat treated at (a) 400 °C (1 h) (b) 400 °C (4 h), fitted into four subspectra. (●, ○, △, □, ▽) Raw spectra, I, II, III, and IV sextets (Table II), respectively.

can be attributed to the Fe_3B phase, thus indicating at least three magnetically inequivalent sites in the crystalline Fe_3B. The precipitated Fe_3B is a metastable phase which can decompose at higher temperatures [1]. The possible decomposition of Fe_3B into Fe_2B and α-Fe can occur only at temperatures much above 400 °C and hence it was not observed by us because our heat treatment for $x = 0$ sample did not go beyond 400 °C. In this respect our findings are in agreement with those observed by Chien *et al.* [21], Sánchez *et al.* [20] and Schaafsma *et al.* [2]. It may also be added that our findings indicate that the intensities of α-Fe and Fe_3B are 24% and 76%, respectively, in the spectrum of the 400 °C (4 h) sample.

3.2.2. $x = 2$

The $x = 2$ sample was heat treated at 300 °C (1 h), 300 °C (2 h), 350 °C (1 h), 350 °C (2 h), 400 °C (1 h), 400 °C (2 h), 475 °C (1 h), and 475 °C (4 h). Mössbauer spectra were recorded at room temperature after each heat treatment of the sample. The computer-fitted spectra are shown in Fig. 3 for the 475 °C (1 h) and 475 °C (4 h) sample. The Mössbauer parameters, obtained from computer analysis, are given in Table III. An immediate observation that can be made from Table II is that, compared to the $x = 0$ sample, the crystallization of $x = 2$ sample starts at a higher (475 °C) temperature. This result suggests that the thermal stability of $Fe_{80}B_{18}Si_2$ increases with the addition of silicon. The analysis of the Mössbauer spectra shows that α-Fe and Fe_3B phases crystallize in the sample heat treated at 475 ° C (1 h) and 475 °C (4 h) with three distinct hyperfine fields for the Fe_3B phases. The values of the internal magnetic field, obtained for the Fe_3B phase for the $x = 2$ sample, support the assignment of the tetragonal (t-Fe_3B) phase (Table III). This conclusion is confirmed by the XRD studies. The relative intensities of the α-Fe and t-Fe_3B phases, observed by us for the $x = 2$ sample, are 20% and 80%, respectively, and thus show little change from the values observed for the $x = 0$ sample.

3.2.3. $x = 8$

This $x = 8$ sample was given heat treatment at the following temperatures: 300 °C (1 h), 300 °C (2 h), 350 °C (1 h), 350 °C (2 h), 400 °C (1 h), 400 °C (2 h), 475 °C (1 h), 475 °C (2 h), 525 °C (1 h), and 525 °C (4 h) and their Mössbauer spectra were recorded at room temperature. Mössbauer parameters of these spectra are listed in Table IV. Mössbauer spectrum for the $x = 8$ sample, heat treated at 475 °C for 1 h, does not show any clear precipitation. The peaks for the α-Fe phase appear to overlap with those due to the amorphous phase while another new phase appears to precipitate. The computer analysis of the sample ($x = 8$), heat treated at 475 °C for 4 h, when fitted into

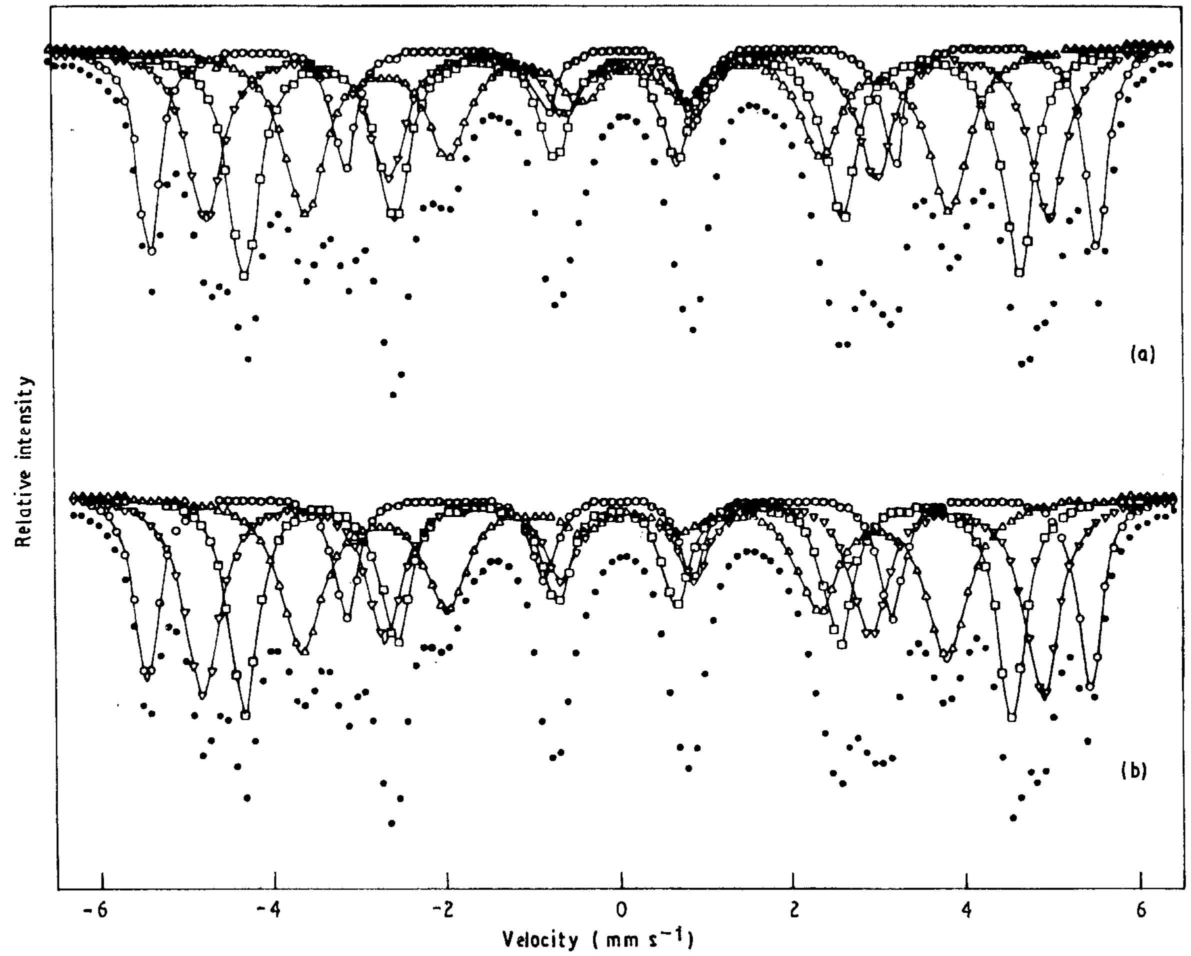

Figure 3 Mössbauer spectra recorded at room temperature of $Fe_{80}B_{18}Si_2$, heat treated at (a) 475 °C (1 h), (b) 475 °C (4 h), fitted into four subspectra. (●, ○, △, □, ▽) Raw spectra, I, II, III, and IV sextets (Table III), respectively.

TABLE III Mössbauer parameters, obtained from computer analysis, for $x = 2$ sample after various heat treatments

Annealing temp. (°C)	Annealing time (h)	IS (mm s^{-1})	H (kOe)	Γ (mm s^{-1})	Remark
300	1	0.10	256	0.92	Amorphous
300	2	0.07	259	0.92	Amorphous
350	1	0.09	259	0.90	Amorphous
350	2	0.07	258	0.92	Amorphous
400	1	0.06	260	0.96	Amorphous
400	2	0.07	260	1.00	Amorphous
475	1	(i) 0.02	332	0.33	α-Fe
		(ii) 0.07	296	0.52	t-Fe_3B
		(iii) 0.13	271	0.42	
		(iv) 0.08	225	0.62	
475	4	(i) 0.00	333	0.34	α-Fe
		(ii) 0.06	297	0.46	t-Fe_3B
		(iii) 0.12	271	0.38	
		(iv) 0.08	227	0.60	

two subspectra, yielded two values of the internal magnetic field (i) $H \simeq 316$ kOe and (ii) $H \simeq 240$ kOe. This computer analysis was complicated due to the partial crystallization which left some material still in the amorphous phase and made least-squares fitting a complicated exercise. The observed value of $H \simeq 316$ kOe is assigned to α-Fe and it appears to be lower than the standard value of $H \simeq 330$ kOe for α-Fe, perhaps because of the presence of the amorphous phase in small amounts. The other subspectrum observed by us yielded $H \simeq 240$ kOe and IS = 0.15 mm s^{-1} and we ascribe it to t-Fe_2B, based on the findings of Takács *et al.* [22].

Mössbauer spectra of the sample heat treated at 525 °C (1 h) and 525 °C (4 h) were analysed in the following two ways:

(i) Model A, in which it was assumed that there are two subspectra arising from α-Fe and Fe_2B phases;

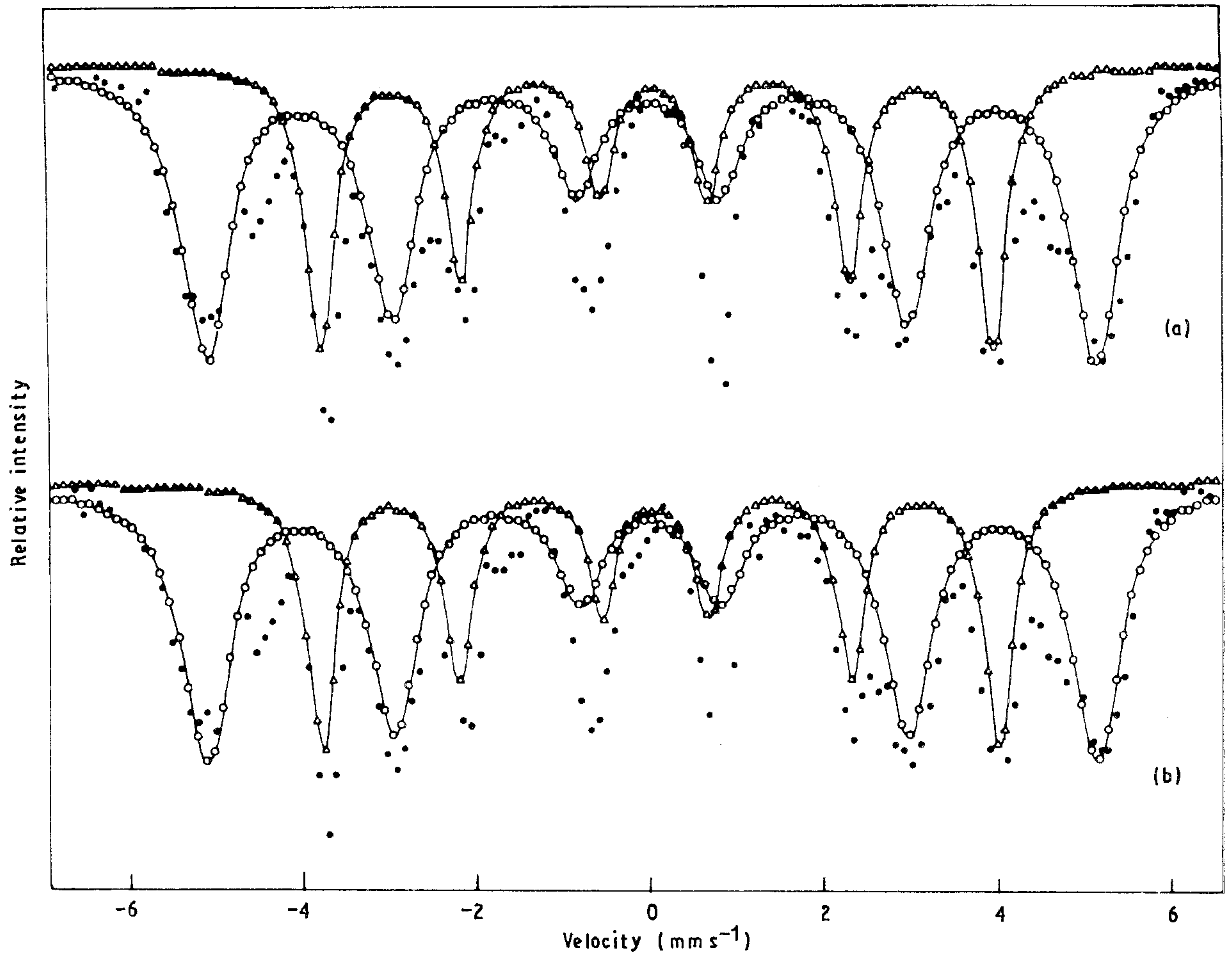

Figure 4 Mössbauer spectra recorded at room temperature of $Fe_{80}B_{12}Si_8$, heat treated at (a) 525 °C (1 h), (b) 525 °C (4 h), fitted using Model A. (●, ○, △) Raw spectra, I, and II sextets (Table IV), respectively.

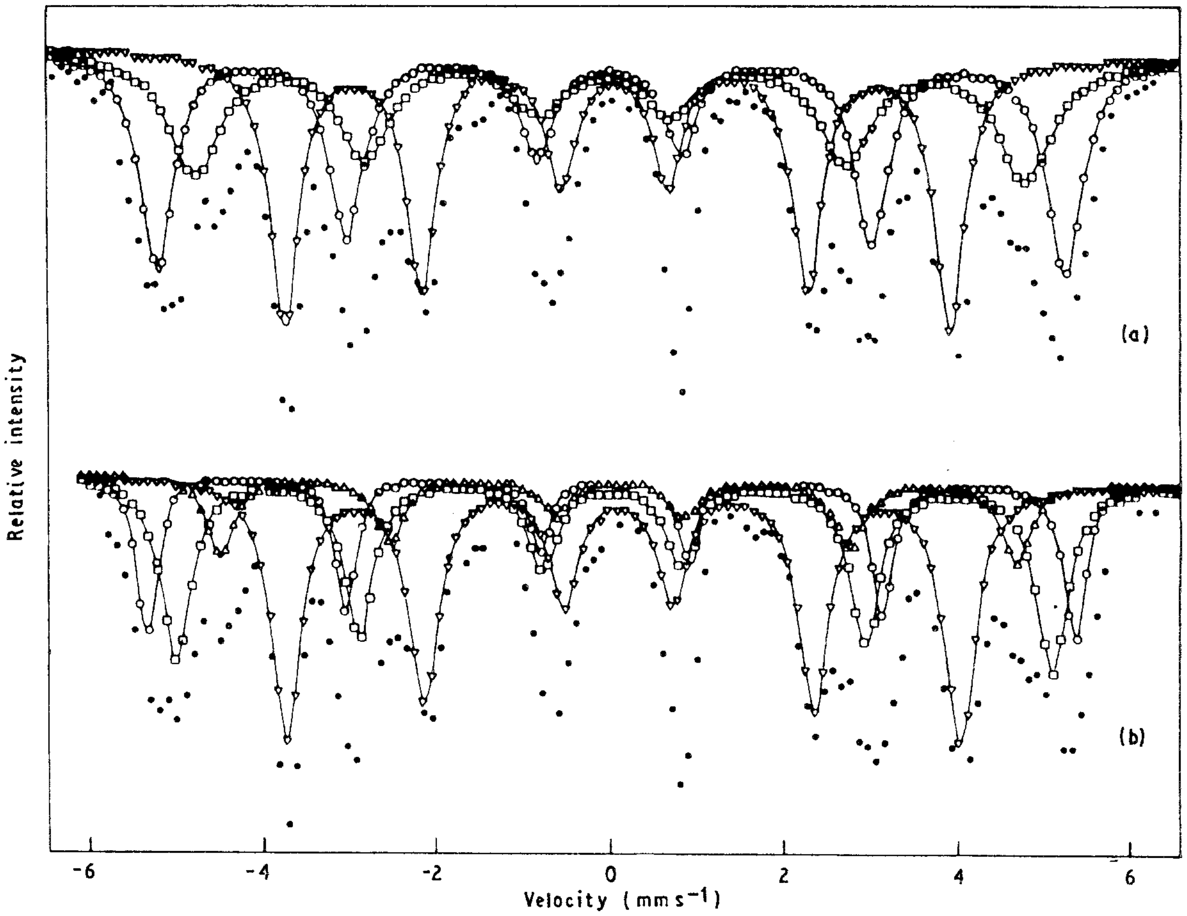

Figure 5 Mössbauer spectra recorded at room temperature of $Fe_{80}B_{12}Si_8$, heat treated at (a) 525 °C (1 h), (b) 525 °C (4 h), fitted using Model B. (●, ○, △, □, ▽) Raw spectra, I, II, III, and IV sextets (Table IV), respectively.

TABLE IV Mössbauer parameters, obtained from computer analysis, for $x = 8$ sample after various heat treatments

Annealing temp. (°C)	Annealing time (h)	IS (mm s^{-1})	H (kOe)	Γ (mm s^{-1})	Remark
300	1	0.13	261	0.93	Amorphous
300	2	0.11	263	0.90	Amorphous
350	1	0.09	262	0.88	Amorphous
350	2	0.10	262	0.88	Amorphous
400	1	0.07	263	0.94	Amorphous
400	2	0.08	264	1.02	Amorphous
475	1	(i) 0.05	316	0.66	Partially crystallized, α-Fe overlapped with amorphous phase
		(ii) 0.15	241	0.40	Fe$_2$B
475	4	(i) 0.05	317	0.68	Partially crystallized, α-Fe overlapped with amorphous phase
		(ii) 0.15	240	0.40	Fe$_2$B
525	1	Model A			
		(i) 0.06	315	0.66	α-Fe
		(ii) 0.14	238	0.38	Fe$_2$B
		Model B			
		(i) 0.06	322	0.48	α-Fe
		(ii) 0.05	295	0.74	(FeSi)
		(iii) 0.14	237	0.42	Fe$_2$B
525	4	Model A			
		(i) 0.04	314	0.66	α-Fe
		(ii) 0.14	239	0.38	Fe$_2$B
		Model B			
		(i) 0.01	327	0.30	α-Fe
		(ii) 0.05	309	0.42	FeSi
		(iii) 0.10	281	0.40	
		(iv) 0.15	238	0.42	Fe$_2$B

(ii) Model B, in which it was assumed that there are more than two subspectra arising from α-Fe, Fe$_2$B and Fe–Si alloy system.

The Mössbauer parameters, obtained from such a computer analysis, are shown in Table IV. The use of Model B was felt necessary because some workers have observed Fe–Si alloy phase during the crystallization of the heat-treated sample of Fe–B–Si system. The present results (Table IV) for the Mössbauer parameters for the 525 °C (1 h) and 525 °C (4 h) treated sample, using Model A, show the clear presence of α-Fe and t-Fe$_2$B phases with the observed H-value ($H = 238$ and 239 kOe) agreeing with the value $H = 236.9$ kOe reported by Takács *et al.* [22] for Fe$_2$B (Fig. 4). The analysis, using Model B, suggests the presence of Fe–Si alloy with $H = 295$ kOe occurring at one Fe site for the 525 °C (1 h) sample and with H = 309 and 281 kOe occurring at two sites for the 525 °C (4 h) sample (Fig. 5). This assignment of Fe–Si alloy phase is based on the results reported in the literature [11, 23].

In order to resolve the choice between Models A and B, we examined the results obtained by the XRD studies. However, these studies did not indicate the presence of the Fe–Si phase in the sample heated at 525 °C (4 h), but this result could be due to a rather small amount of precipitation of the Fe–Si phase.

It is observed from our Mössbauer studies that $x = 0$, 2 and 8 samples, when annealed at various temperatures (Table II, III and IV) show a slight increase in the value of H (internal magnetic field). The atomic arrangements become more ordered with annealing. This increase of atomic ordering can strengthen the long-range exchange interactions responsible for the ferromagnetism of these alloys [21]. This might explain the slight increase in the value of H.

4. Conclusion

Mössbauer spectroscopic studies of the as-received samples of Fe$_{80}$B$_{20-x}$Si$_x$ (x = 0, 2 and 8) indicate that the internal magnetic field increases slightly with x. Similarly, the isomer shift increases with the addition of silicon and it can be understood in terms of a charge-transfer model. Mössbauer spectroscopic and X-ray diffraction studies of heat-treated samples show that the crystallization of the $x = 0$ and 2 samples leads to α-Fe and t-Fe$_3$B. In the case of the $x = 8$ sample, however, the final crystallized phases are found to be α-Fe and t-Fe$_2$B (instead of Fe$_3$B), and perhaps Fe–Si. Addition of silicon to the Fe–B system increases the crystallization temperature thus improving the thermal stability of the system.

Acknowledgements

We are grateful to Dr F.E. Luborsky for providing the samples and to Professor A.K. Majumdar for useful discussions.

References

1. T. KEMÉNY, I. VINCZE, B. FOGARASSY and SIGURDS ARAJS, *Phys. Rev. B* **20** (1979) 476.
2. A. S. SCHAAFSMA, H. SNIJDERS, F. VAN DER WOUDE, J. W. DRIJVER and S. RADELAAR, *ibid.* **20** (1979) 4423.
3. M. W. RUCKMAN, R. A. LEVY, A. KESSLER and R. HASEGAWA, *J. Non-Cryst. Solids* **40** (1980) 393.
4. H. N. OK and A. H. MORRISH, *Phys. Rev. B* **22** (1980) 3471.
5. J. A. CUSIDÓ A. ISALGUÉ, and J. TEJADA, *Phys. Status Solidi* **A87** (1985) 169.
6. H. N. OK and A. H. MORRISH, *J. Phys.* **11** (1981) 1495.
7. H. N. OK, K. S. BAEK, and C. S. KIM, *Phys. Rev. B* **24** (1981) 6600.
8. I. W. DONALD, T. KEMÉNY, and H.A. DAVIES, *J. Phys. F* **11** (1981) L31.
9. T. MASUMOTO, H. KIMURA, A. INOUE, and Y. WASEDA, *Mater Sci. Engng* **23** (1976) 141.
10. ANIL K. BHATNAGAR and N. RAVI, *Phys. Rev. B* **28** (1983) 359.
11. T. NAGARAJAN, U. CHIDAMBARAM ASARI, S. SRINIVASAN, V. SRIDHARAN and A. NARAYANASAMY, *Mater. Sci. Engng.* **97** (1988) 355.
12. GHEOREHE ILONCA and VIOREL FLORESCU, *ibid.*, **99** (1988) 43.
13. I. NOWIK, I. FELNER, Y. WOLFUS, and Y. YESHURUN, *J. Phys. F* **18** (1988) L181.
14. RITA SINGHAL and A. K. MAJUMDAR, *Phys. Rev. B* **44** (1991) 2673.
15. RITA SINGHAL, PhD thesis, Indian Institute of Technology, Kanpur (1991), unpublished.
16. L. R. WALKER, G. K. WERTHEIM and V. JACCARINO, *Phys. Rev. Lett.* **6** (1961) 98.
17. M. TANIWAKI and M. MAEDA, *Mater. Sci. Engng.* **99** (1988) 47.
18. U. GONSER, M. GHAFARI, M. ACKERMANN, H. P. KLEIN, J. BAUER, and H. -G. WAGNER, in "Proceedings of the 4th International Conference on Rapidly Quenched Metals, " edited by T. Masumoto and K. Sujuki (The Japan Institute of Metals, Sendai, 1982) p.639.
19. G. LE. CAER and J. M. DUBOIS, *Phys. Status Solidi* **A64** (1981) 275.
20. F. H. SÁNCHEZ, Y. D. ZHANG, J. I. BUDNICK and R. HASEGAWA, *J. Appl. Phys.* **66** (1969) 1671.
21. C. L. CHIEN, D. MUSSER, E. M. GYORGY, R. C. SHERWOOD, H. S. CHEN, F. E. LUBORSKY and J. L. WALTER, *Phys. Rev. B* **20** (1979) 283.
22. L. TAKÁCS, M. C. CADEVILLE and I. VINCZE, *J. Phys. F* **5** (1975) 800.
23. L. HÄGGSTRÖM, L. GRANÄS, R. WÄPPLING, and S. DEVANARAYANAN, *Phys. Scr.* **7** (1973) 125.

Received 15 October 1991
and accepted 18 March 1992